

A Comparison of ACE Measurements of Galactic Cosmic-Ray Abundances and Energy Spectra for Two Successive Solar Minima

K. A. Lave*, W. R. Binns*, A. C. Cummings[†], G. A. de Nolfo[‡], M. H. Israel*, R. A. Leske[†],
R. A. Mewaldt[†], E. C. Stone[†], T. T. von Rosenvinge[‡], and M. E. Wiedenbeck[§]

*Department of Physics & McDonnell Center for Space Sciences, Washington Univ., St. Louis, MO 63130 USA

[†]California Institute of Technology, Pasadena, CA 91125 USA

[‡]NASA Goddard Space Flight Center, Greenbelt, MD 20771 USA

[§]Jet Propulsion Laboratory, California Institute of Technology, Pasadena, CA 91109 USA

Abstract. Using current solar minimum measurements from the Cosmic Ray Isotope Spectrometer (CRIS) onboard the Advanced Composition Explorer (ACE), we report the observed elemental abundances and energy spectra for C, O, Si, and Fe in the energy range of ~ 50 -500 MeV/nucleon. These measurements are compared to prior CRIS observations for the 1997-98 solar minimum period, when the solar magnetic field was of the opposite polarity. By April 2009, the current solar minimum intensities for each of the four elements has surpassed the peak intensities observed during the previous solar minimum. We also examine the correlation of the galactic cosmic-ray intensities with the tilt angle of the heliospheric current sheet. These studies will be important for understanding solar modulation processes, such as changes in drift effects during a solar cycle.

Keywords: cosmic rays — **Galaxy:** abundances — **Sun:** activity

I. INTRODUCTION

The Cosmic Ray Isotope Spectrometer (CRIS [1]) onboard NASA's *Advanced Composition Explorer* (ACE) allows for high statistics observations of galactic cosmic-ray (GCR) nuclei arriving near Earth. Studies of the composition and energy spectra of GCRs provide information about nucleosynthetic processes occurring at the source, as well as their acceleration and transport through the Galaxy. Although we can not directly measure cosmic rays outside of the heliosphere, measurements of the local energy spectra during the minimum phase of solar activity offer the best glimpse of the interstellar cosmic-ray spectra.

Since its launch on August 25, 1997, CRIS has continuously observed GCRs during two successive solar minimum periods. During this time, the polarity of the Sun's magnetic field has changed from $A > 0$ to $A < 0$, causing a reversal in the drift direction of the nuclei along the heliospheric current sheet. High precision studies of GCRs during both of these polarity epochs will be important for the refinement of solar modulation models that include drift effects.

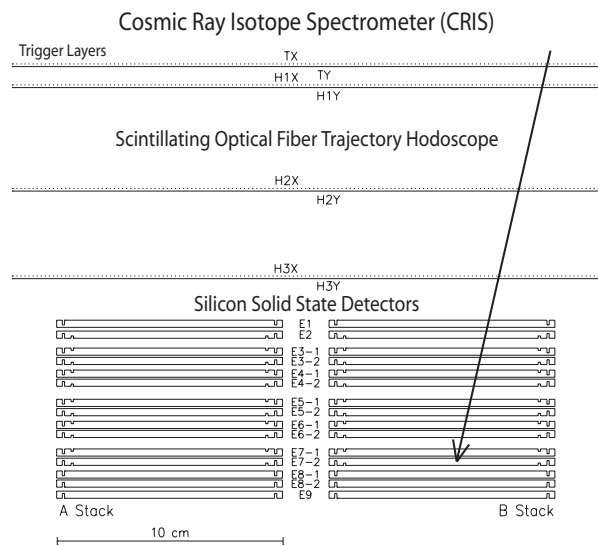


Fig. 1: CRIS instrument (with two of the four detector stacks shown). The arrow represents an incident particle stopping in the bottom of detector E7.

In this study, we present CRIS GCR energy spectra and relative abundances for C, O, Si, and Fe for energies between 50 and 500 MeV/nucleon during two successive periods of solar minimum. The first period includes data taken between August 28, 1997 and April 19, 1998 during the $A > 0$ epoch. The second period includes data taken between January 16, 2008 and April 18, 2009, during the $A < 0$ epoch. We also show the time evolution of the intensity of GCR Fe and compare the observations to the tilt angle of the heliospheric current sheet [2].

II. CRIS INSTRUMENT

The CRIS instrument consists of four silicon solid-state-detector stacks, each of which contains nine circular silicon detectors (see Figure 1). Trajectories through these detectors are measured using the square scintillating optical fiber trajectory (SOFT) hodoscope composed of three x - y tracking layers, with an additional set of layers serving as a trigger. The charge and mass of particles that stop in the silicon detectors are determined using the total energy deposited (E' in MeV) in the stop

Element	Energies (MeV/nucleon)						
	1997–1998 Intensities [10^{-9} (cm ² s sr MeV/nucleon) ⁻¹]						
	2008–2009 Intensities [10^{-9} (cm ² s sr MeV/nucleon) ⁻¹]						
C	68.2	91.5	117.2	139.4	159.4	177.7	194.8
	517.6	616.0	714.9	759.8	797.7	816.8	795.1
	$\pm 3.8 \pm 14.9$	$\pm 3.4 \pm 18.3$	$\pm 4.2 \pm 22.3$	$\pm 4.9 \pm 25.1$	$\pm 5.6 \pm 28.1$	$\pm 6.2 \pm 30.8$	$\pm 6.4 \pm 32.2$
	$\pm 2.7 \pm 15.3$	$\pm 2.3 \pm 18.6$	$\pm 2.9 \pm 22.9$	$\pm 3.4 \pm 25.3$	$\pm 3.9 \pm 28.8$	$\pm 4.3 \pm 31.2$	$\pm 4.4 \pm 33.0$
O	80.3	107.9	138.4	164.9	188.8	210.6	231.1
	573.6	664.9	735.9	770.3	775.5	799.9	756.7
	$\pm 3.7 \pm 16.6$	$\pm 3.2 \pm 19.9$	$\pm 3.9 \pm 23.2$	$\pm 4.4 \pm 26.2$	$\pm 5.0 \pm 28.3$	$\pm 5.5 \pm 31.8$	$\pm 5.6 \pm 32.9$
	$\pm 2.6 \pm 16.8$	$\pm 2.2 \pm 20.4$	$\pm 2.7 \pm 24.1$	$\pm 3.1 \pm 26.9$	$\pm 3.5 \pm 29.6$	$\pm 3.9 \pm 32.8$	$\pm 4.0 \pm 34.6$
Si	109.9	148.2	191.0	228.4	262.3	293.6	323.1
	91.9	104.6	110.9	111.9	112.9	110.4	103.4
	$\pm 1.3 \pm 2.7$	$\pm 1.1 \pm 3.2$	$\pm 1.3 \pm 3.7$	$\pm 1.4 \pm 4.2$	$\pm 1.6 \pm 4.6$	$\pm 1.8 \pm 5.0$	$\pm 1.8 \pm 5.1$
	$\pm 0.9 \pm 2.8$	$\pm 0.8 \pm 3.3$	$\pm 0.9 \pm 3.9$	$\pm 1.0 \pm 4.3$	$\pm 1.1 \pm 4.8$	$\pm 1.2 \pm 5.2$	$\pm 1.3 \pm 5.5$
Fe	150.2	204.2	265.0	318.6	367.8	413.4	456.9
	68.7	73.8	73.9	69.3	68.0	62.5	59.5
	$\pm 0.9 \pm 2.1$	$\pm 0.8 \pm 2.4$	$\pm 0.9 \pm 2.7$	$\pm 1.0 \pm 3.0$	$\pm 1.1 \pm 3.3$	$\pm 1.1 \pm 3.4$	$\pm 1.2 \pm 3.6$
	$\pm 0.7 \pm 2.3$	$\pm 0.5 \pm 2.6$	$\pm 0.6 \pm 3.0$	$\pm 0.7 \pm 3.3$	$\pm 0.8 \pm 3.6$	$\pm 0.8 \pm 3.8$	$\pm 0.8 \pm 4.0$

TABLE I: CRIS solar minimum intensities. Listed below each intensity are the statistical (first uncertainty) and systematic (second uncertainty) contributions to the total uncertainty.

detector and multiple measurements of the rate of energy loss (dE/dx in MeV g⁻¹ cm²) in the prior detectors (see [1] and [3] for more information). Knowing the charge and mass, as well as the amount of material that a particle traverses prior to the detector in which it stops (corrected for the angle of incidence), we may calculate the final depth of a particle in the stop detector using the semi-empirical range-energy relations for hydrogen [4], scaled to heavy-ions [5].

The bottom (E9) detector in each stack is used to identify those particles that do not stop within the previous eight detectors, while annular guard rings reject particles that exit the detector sides. Valid events were defined to be those that have incident angles $\leq 30^\circ$ from the normal that stop in detectors E2-E8 without passing too close (within 0.5 mm) to the edge of the stack. Particles must not have a calculated stop depth within 160 μm of the top or bottom face of a detector to avoid silicon detector “dead layers”.

III. ELEMENTAL SPECTRA

Figure 2 shows the elemental energy spectra for C, O, Si, and Fe for the two solar minimum periods, with HEAO-3 data [6] given for reference. The CRIS data shown in this figure are given in Table I. These spectra have been corrected for livetime, geometrical acceptance, energy intervals, and detector efficiencies. Also included in Figure 2 are the results of a steady-state leaky box propagation calculation (e.g., [7]), combined with a solar modulation model based on a numerical solution of the spherically symmetric Fisk model [8] using a modulation level of $\phi = 325$ MV, representative of the 1997-98 solar minimum. The HEAO-3 data, which are best fit with a modulation level of $\phi = 750$ MV [3], have been adjusted to the CRIS modulation level by taking ratios of the model curves to determine the

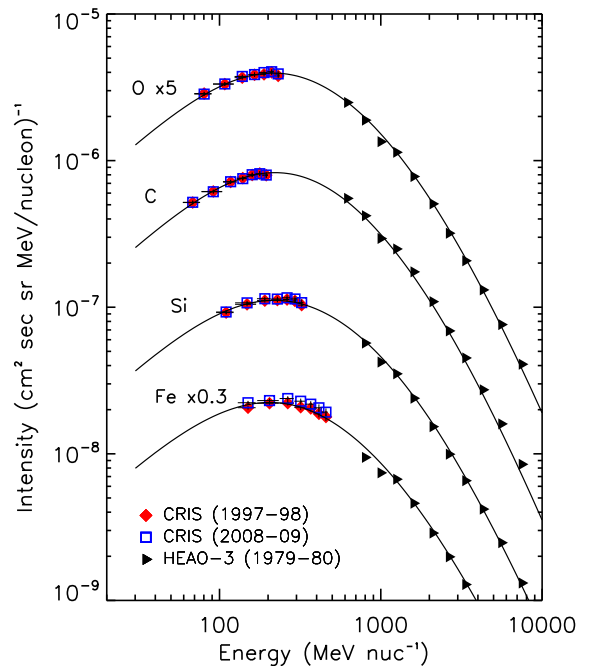


Fig. 2: Comparison of the elemental energy spectra for 1997-98 (filled diamonds) and 2008-09 (open squares). Higher energy HEAO-3 data (filled triangles) are shown for reference. A propagation model calculation (solid curves) corresponding to a solar modulation level of $\phi = 325$ MV is also shown. The HEAO-3 data have been adjusted to this modulation level.

energy-dependent correction factors. This propagation model gives a good fit to both the 1997-98 CRIS data and the HEAO-3 data.

Contributions to the systematic uncertainties in the

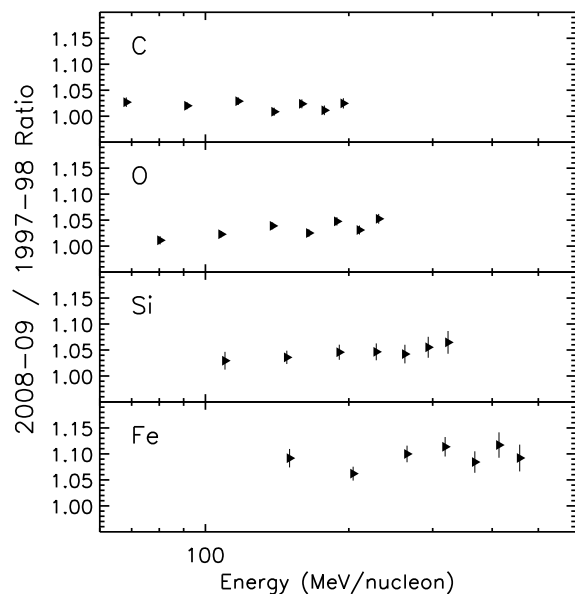


Fig. 3: Ratios of the CRIS solar minimum spectra. Only statistical uncertainties are shown.

CRIS measurements arise from corrections for fragmentation in the instrument, hodoscope efficiency, and the geometry factor. The plotted errors in the measurements are then the quadratic sum of the systematic and statistical uncertainties. The four elements examined in this paper are among the most abundant species observed by CRIS, and therefore the statistical uncertainties are quite small (for example, $\sim 0.6\%$ for O in each range in 1997-98).

Ratios between the two different CRIS solar minimum spectra are shown in Figure 3. The 2008-09 C intensities increased by $\sim 1\text{-}3\%$ compared to the 1997-98 intensities, O increased by $\sim 1\text{-}5\%$, Si increased by $\sim 3\text{-}6\%$, and Fe increased by $\sim 6\text{-}12\%$. These increases demonstrate that during solar minima, GCRs do not always exhibit the same energy spectra, and quantitatively the changes are not identical for all cosmic-ray species.

IV. COMPOSITION

The CRIS relative GCR abundances for both solar minimum periods were taken at 160 MeV/nucleon and are given in Table II, normalized to $\text{Si} \equiv 1000$. This energy was chosen because of its overlap with measurements of the four elements. Relative abundances were calculated by fitting the energy spectra with a parabola in $\log(\text{Intensity})$ versus $\log(\text{Energy/nucleon})$ and taking ratios of the curves at 160 MeV/nucleon. Statistical uncertainties are based on the total number of counts, and are listed in the table. The systematic uncertainties are larger than the statistical contributions for each of these elements, but they tend to cancel when comparing with nearby elements, so they are not included in the table.

Compared to the 1997-98 data, the C abundance relative to Si for the current solar minimum has decreased by $\sim 2\%$, while the Fe abundance relative to Si has increased by $\sim 4.5\%$. This reflects the previous observation that the higher-Z elements exhibit larger increases in the absolute intensities. The differences among the elements likely reflect differences in their interstellar spectra [3] and small differences in the adiabatic cooling effects during $A < 0$ and $A > 0$. Silicon absolute intensities provided in the table may be used to determine the intensities of the four elements at 160 MeV/nucleon.

Element	Relative Abundance	
	1997-1998	2008-2009
C	7337.0 ± 18.4	7202.8 ± 12.3
O	7082.6 ± 16.0	7069.1 ± 10.8
Si	1000.0 ± 5.0	1000.0 ± 3.3
Fe	653.7 ± 3.5	683.0 ± 2.4

Element	Absolute Intensity	
	$10^{-9} [\text{cm}^2 \text{ s sr MeV/nucleon}]^{-1}$	
Si	107.4 ± 3.3	111.4 ± 3.4

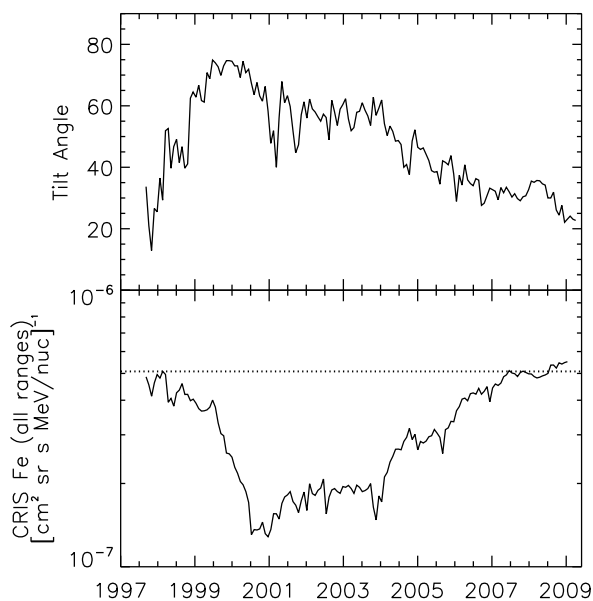
TABLE II: Solar minimum relative abundances at 160 MeV/nucleon. Values are normalized to $\text{Si} \equiv 1000$. Only statistical uncertainties are given for the abundances.

V. COMPARISON WITH TILT ANGLE

Since the interstellar GCR spectra are modulated upon entering the heliosphere, it is useful to compare the local energy spectra to measured characteristics of the interplanetary medium. Such studies are important for understanding solar modulation properties and should ultimately lead to better models. We have chosen to compare the CRIS Fe intensities, which have exhibited the largest increases since the 1997-98 solar minimum, with the average tilt angle of the heliospheric current sheet (HCS) as measured by the Wilcox Solar Observatory [2] using their “classic” model. The results are plotted in Figure 4, with the Fe data representing the intensity summed over all ranges (E2-E8). All data are averaged over solar rotation.

From this plot we see that the peak Fe intensity of the 1997-98 solar minimum, indicated by the dotted line, was reached by the middle of 2007. At this time, the HCS tilt angle was still elevated, at around 30° . By comparison, the previous solar minimum saw tilt angles $< 10^\circ$ between late 1995 and early 1996 (not shown in Figure 4). A noticeable increase ($\sim 8\%$) in the Fe intensity is also seen near the end of 2008, which approximately coincides with a decrease in the tilt angle.

During the previous solar minimum ($A > 0$), low-energy GCRs drifted downward from the polar regions of the heliosphere and outward along the HCS. For the present $A < 0$ epoch, positive ions drift inward along the HCS, making the tilt of the HCS an important factor in determining the level of solar modulation. As the tilt angle decreases, the distance along the wavy HCS becomes shorter, facilitating the inward drift of ions and producing an increased intensity at 1 AU [9]. As a result,



..

Fig. 4: Comparison of the tilt angle of the heliospheric current sheet and the CRIS Fe intensities, summed over all ranges. Data are given as solar rotation averages. The dotted line indicates the peak Fe intensity reached during the 1997-98 solar minimum.

we expect to see a further increase in the intensity for the present solar minimum if the HCS continues to drop to lower tilt angles (see also [10]).

VI. SUMMARY

We have presented the energy spectra and relative abundances for C, O, Si, and Fe during the 1997-98 and 2008-09 solar minima using the CRIS instrument.

These data have been used to show the differences in the modulation of GCRs during two different solar magnetic epochs. We have found that the intensities are larger now than during the previous solar minimum, with the largest changes observed in the Fe intensities.

Additionally, we have compared the CRIS Fe data to the tilt angle of the heliospheric current sheet and have found that the lower tilt angle is correlated with the increased intensity in the present solar minimum. We expect further increases in the Fe intensity for the current solar minimum, should the tilt angle continue to decrease. Future work should be carried out to determine whether the tilt angle and the polarity of the Sun's magnetic field are responsible for differences in the GCR intensities observed near Earth between different solar minima. Studies such as these are useful for developing sophisticated solar modulation models that include information specific to the period of solar activity, such as the drift direction of particles traveling in the heliosphere.

ACKNOWLEDGEMENTS

This research is supported by NASA at Caltech, WU, JPL, and GSFC under grant NNX08AI11G. KL would also like to thank NASA for support under grant NNX07AP22H.

REFERENCES

- [1] E. C. Stone, et al., *Sp. Sci. Rev.*, 86, 285, 1998.
- [2] J. T. Hoeksema, *Sp. Sci. Rev.*, 72, 137, 1995.
- [3] J. S. George, et al., *ApJ*, 2009 (in press).
- [4] H. H. Andersen & J. F. Ziegler, *The Stopping Powers and Ranges of Ions in Matter*, Vol. 3 (New York: Pergamon), 1977.
- [5] S. P. Ahlen, *Rev. Mod. Phys.*, 52, 121, 1980.
- [6] J. J. Engelmann, et al., *A&A*, 233, 96, 1990.
- [7] M. Meneguzzi, J. Audouze, & H. Reeves, *A&A*, 15, 337, 1971.
- [8] L. A. Fisk, *JGR*, 76, 221, 1971.
- [9] J. A. Le Roux & M. S. Potgieter, *ApJ*, 361, 275, 1990.
- [10] R. Mewaldt, R. Leske, K. Lave, & M. Wiedenbeck, *Cosmic-Ray Fe Intensity Reaches Record Levels in 2008-2009*, <http://www.srl.caltech.edu/ACE/ACENews122.html>.